

Reactive oxygen species stimulate mitochondrial allele segregation toward homoplasmy in human cells

Feng Ling^{a,b,*}, Rong Niu^{a,b}, Hideyuki Hatakeyama^{b,c}, Yu-ichi Goto^{b,c}, Takehiko Shibata^{b,d,*}, and Minoru Yoshida^{a,b}

^aChemical Genetics Laboratory and ^dCellular and Molecular Biology Laboratory, RIKEN, Saitama 351-0198, Japan; ^bJapan Agency for Medical Research and Development–Core Research for Evolutional Science and Technology, Tokyo 100-0004 Japan; ^cDepartment of Mental Retardation and Birth Defect Research, National Center of Neurology and Psychiatry, Tokyo 187-8502, Japan

ABSTRACT Mitochondria that contain a mixture of mutant and wild-type mitochondrial (mt) DNA copies are heteroplasmic. In humans, homoplasmy is restored during early oogenesis and reprogramming of somatic cells, but the mechanism of mt-allele segregation remains unknown. In budding yeast, homoplasmy is restored by head-to-tail concatemer formation in mother cells by reactive oxygen species (ROS)–induced rolling-circle replication and selective transmission of concatemers to daughter cells, but this mechanism is not obvious in higher eukaryotes. Here, using heteroplasmic m.3243A > G primary fibroblast cells derived from MELAS patients treated with hydrogen peroxide (H₂O₂), we show that an optimal ROS level promotes mt-allele segregation toward wild-type and mutant mtDNA homoplasmy. Enhanced ROS level reduced the amount of intact mtDNA replication templates but increased linear tandem multimers linked by head-to-tail unit-sized mtDNA (mtDNA concatemers). ROS-triggered mt-allele segregation correlated with mtDNA-concatemer production and enabled transmission of multiple identical mt-genome copies as a single unit. Our results support a mechanism by which mt-allele segregation toward mt-homoplasmy is mediated by concatemers.

Monitoring Editor

Donald D. Newmeyer
La Jolla Institute for Allergy
and Immunology

Received: Oct 6, 2015

Revised: Mar 14, 2016

Accepted: Mar 16, 2016

INTRODUCTION

Eukaryotic cells generally contain hundreds to thousands of copies of mitochondrial DNA (mtDNA). Mutations occur in mtDNA much more frequently than in nuclear genomic DNA; therefore the mitochondrial genome tends toward heteroplasmy, a state associated

with mitochondrial disorders, aging, and various human diseases (Holt *et al.*, 1988; Linnane *et al.*, 1989; Wallace, 1994; Ozawa, 1997; Smeitink *et al.*, 2006). In humans, one common heteroplasmic mtDNA mutation is the A-to-G transition at nucleotide position (np) 3243 (m.3243A > G), which forms stable heteroplasmy with wild-type mtDNA (Lehtinen *et al.*, 2000; Raap *et al.*, 2012) and causes mitochondrial myopathy, encephalopathy, lactic acidosis, and stroke-like episodes (MELAS) disease (Goto *et al.*, 1990) and diabetes (Reardon *et al.*, 1992; Kadowaki *et al.*, 1994). The onset of pathogenic mtDNA-associated diseases depends on an increase in the ratio of mutant to wild-type mtDNA in specific tissues. Mechanisms underlying maintenance of (and alterations in) the proportion of mutant mtDNA in heteroplasmic cells are of considerable clinical importance; however, it remains unclear how mt-allele segregation occurs in higher eukaryotes.

Rapid segregation of mtDNA heteroplasmy to homoplasmy (in which all mtDNA copies have an identical sequence) occurs during early oogenesis in metazoan female germlines and is known as the bottleneck phenomenon (Cree *et al.*, 2008; Khrapko, 2008; Wai *et al.*, 2008). A similar phenomenon was observed during reprogramming of somatic cells (Fujikura *et al.*, 2012). The dominant molecular

This article was published online ahead of print in MBoC in Press (<http://www.molbiolcell.org/cgi/doi/10.1091/mbc.E15-10-0690>) on March 23, 2016.

*Address correspondence to: Feng Ling (ling@postman.riken.go.jp), Takehiko Shibata (tshibata@postman.riken.go.jp).

Abbreviations used: ACTB, nuclear β -actin gene; BrdU, bromodeoxyuridine; cc, closed circular; CM-H2DCFDA, 5-(and-6)-chloromethyl-2,7-dichlorodihydrofluorescein diacetate acetyl ester; concatemers, linear tandem multimers linked by head-to-tail unit-sized mtDNA; 2D, two-dimensional; EtBr, ethidium bromide; ETC, electron transport chain; ExoIII, exonuclease III; m.3243A>G, mtDNA mutation of the A-to-G transition at nucleotide position (np) 3243; MELAS, mitochondrial myopathy, encephalopathy, lactic acidosis, and stroke-like episodes; mt, mitochondrial; NAC, N-acetylcysteine; oc, open-circular; PBS, phosphate-buffered saline; PFGE, pulsed-field gel-electrophoresis; POLG, mtDNA polymerase γ ; ROS, reactive oxygen species; TAE, Tris-acetate-EDTA; TBE, Tris-boric-EDTA.

© 2016 Ling *et al.* This article is distributed by The American Society for Cell Biology under license from the author(s). Two months after publication it is available to the public under an Attribution–Noncommercial–Share Alike 3.0 Unported Creative Commons License (<http://creativecommons.org/licenses/by-nc-sa/3.0>).

“ASCB®,” “The American Society for Cell Biology®,” and “Molecular Biology of the Cell®” are registered trademarks of The American Society for Cell Biology.

species of human mtDNA is the circular monomer (one genome unit in size), which replicates by a θ -type mechanism and randomly assorts into sister cells. However, θ -type replication and inheritance cannot explain the rapid segregation of mt-alleles observed in heteroplasmic mammalian cells (Hauswirth and Laipis, 1982; Ashley *et al.*, 1989; Koehler *et al.*, 1991) and single-celled organisms (Birky, 1978a,b). Mathematical modeling predicted that decreasing the number of mtDNA-segregating units to a few copies promotes the segregation of mt-alleles (Birky, 1978a,b). One proposed explanation is a genetic bottleneck, in which mtDNA copy number is dramatically reduced, although the nature (and existence) of such a mechanism remains controversial (Cao *et al.*, 2007; Cree *et al.*, 2008; Khrapko, 2008; Wai *et al.*, 2008). Another mechanism that we found in *Saccharomyces cerevisiae* is vegetative segregation of mt-alleles caused by formation of head-to-tail tandem multimers (concatemers) of single genome-sized mtDNA in mother cells and their selective transmission into daughter cells.

Concatemers are produced by reactive oxygen species (ROS)-triggered rolling-circle replication, allowing for inheritance of multiple mtDNA genome units as a single segregation unit, thereby allowing most progeny cells to become homoplasmic within eight generations of growth from a heteroplasmic ancestor cell (Ling and Shibata, 2002, 2004; Ling *et al.*, 2011). However, it remains unclear whether ROS production contributes to the segregation of mt-alleles in human cells despite the established role for H₂O₂ as a signaling molecule in yeast, plants, and animals (Kamata and Hirata, 1999; Neill *et al.*, 2002; Bienert *et al.*, 2006; Ling *et al.*, 2011). In addition, selective mtDNA-concatemer transmission from mother to daughter cells clearly explains homoplasmy restoration in budding yeast and asymmetric cell division, but it is unclear whether this mechanism is applicable to most organisms, including humans, that undergo symmetric cell division.

In this study, using heteroplasmic m.3243A > G primary fibroblast cell lines derived from MELAS patients, we provide evidence that ROS triggers rolling-circle replication, which forms concatemers and stimulates mtDNA-allele segregation toward homoplasmy during vegetative growth.

RESULTS

Induced mt-allele segregation by ROS

To test the effects of ROS on mt-allele segregation, we analyzed the m.3243A > G mutant fraction in clones from H₂O₂-treated heteroplasmic fibroblast cells derived from MELAS patients (Supplemental Figure S1). Treatment-induced changes to the distribution of mutant mtDNA-allele fractions from a single-peaked to a bimodal distribution (Figure 1A, parental to i) are achieved only by mt-allele segregation from heteroplasmic cells to homoplasmic descendants. A shift of the distribution toward the wild-type or mutant mtDNA side results from selection for cells with either wild-type or mutant mtDNA (Figure 1A, parental to ii and iii, respectively).

MELAS cells treated with H₂O₂ followed by 6 d of cultivation ("posttreatment cultivation") were subjected to single-cell cloning, and the m.3243A > G mutant fraction in each clone was analyzed (Supplemental Figure S1B). Treatment of cells with H₂O₂ caused detectable increases in intracellular ROS levels within 15 min (Figure 1B). The m.3243A > G mutant fraction among all mtDNAs within each cell clone was measured using an established PCR-restriction fragment-length polymorphism (RFLP) assay (diagram in Supplemental Figure S1A, left; Goto *et al.*, 1990).

The original MELAS cell culture consisted of cells with 32 ± 3% (*n* = 5) m.3243A > G mutant mtDNA (Supplemental Figure S1A, right), and all clones isolated from untreated MELAS culture con-

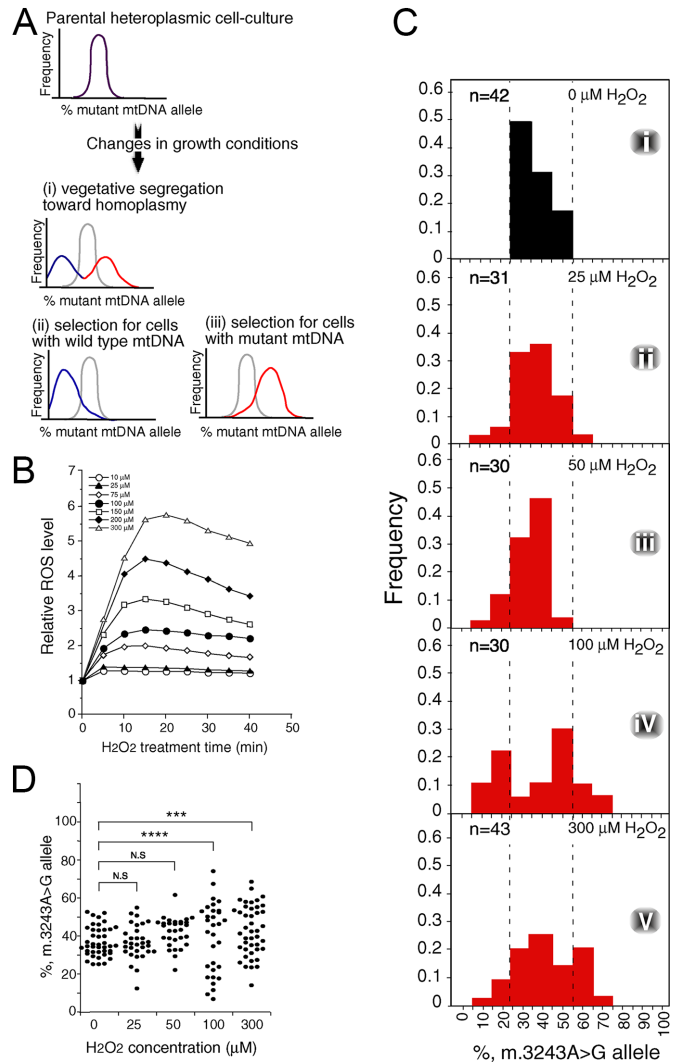


FIGURE 1: Elevated ROS levels induced segregation of mtDNA alleles in heteroplasmic MELAS cells. (A) Possible distribution profile shifts from parental heteroplasmic cells after growth condition changes. (i) Vegetative segregation toward homoplasmy. (ii) Selection for cells with normal mtDNA. (iii) Selection for cells with mutant mtDNA. (B) Intracellular ROS level after H₂O₂ treatment. MELAS cells were treated with the indicated concentrations of H₂O₂ and measured at 5-min intervals using the probe CM-H₂DCFDA. (C) Distribution of m.3243A > G mutant fraction in clones derived from cells treated for 30 min with (i) 0, (ii) 25 μM, (iii) 50 μM, (iv) 100 μM, or (v) 300 μM H₂O₂ and then cultivated to allow robust growth of cells. (D) Statistical analysis for distribution of the m.3243A > G mutant fraction in clones derived from cells treated with the indicated concentrations of H₂O₂. ****p* < 0.001, *****p* < 0.0001; N.S., not significant. For each concentration of H₂O₂, the treatment time was 30 min.

tained m.3243A > G mutant fractions within a range of 25–55% (Figure 1, Ci and D, and Supplemental Figure S2A). Treatment with 100 μM H₂O₂ for 30 min caused ~40% of the clone population to yield colonies with <25% or >55% m.3243A > G mutant allele content (Figure 1, Civ and D). The shift to a bimodal distribution is indicative of mt-allele segregation (Figure 1Ai). Remarkably, sequencing revealed that some clones (such as clone 1) derived from MELAS cells treated with 100 μM H₂O₂ for 30 min and cultivated for 6 d contained a very low (<3%) m.3243A > G mtDNA level (Supplemental Figure S2F).

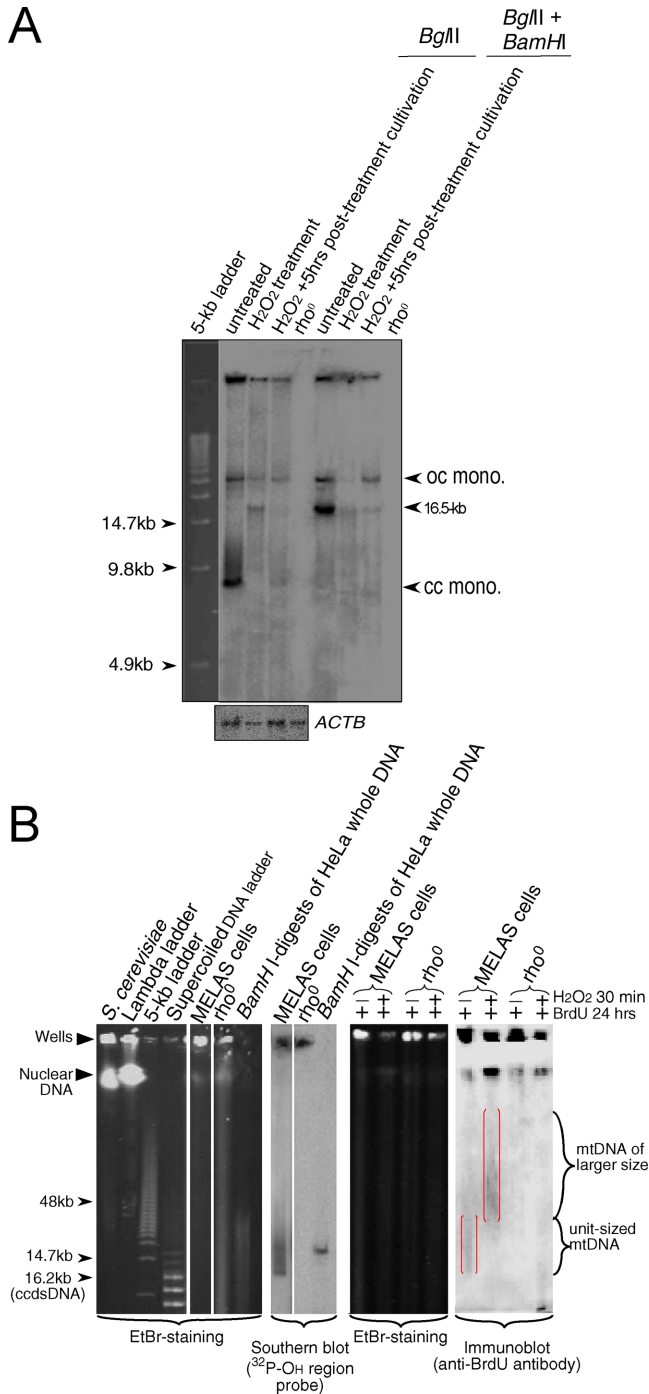


FIGURE 2: Analyses of mtDNA-species in H₂O₂-treated MELAS cells. (A) One-dimensional gel analyses. The *Bgl*II or *Bgl*II/*Bam*HI digests were separated on a 0.5% agarose gel by electrophoresis. Treatment with *Bgl*II (no cutting site on human mtDNA) slightly reduced background signals from nuclear genomic DNA. Signals from mtDNA species were detected by Southern hybridization using a ³²P-labeled mtDNA fragment of the O_H region as a probe. Signals from the nuclear gene ACTB are shown below the one-dimensional gel profile. Open-circular monomers migrated more slowly than linear monomers (lane 1) and were resistant to *Bam*HI treatment (lane 5). Because the *Bam*HI cutting site in human mtDNA is located close to the heavy chain replication origin (*ori*H) within the D-loop region, mtDNA replicating in the θ-type mode with the D-loop are *Bam*HI resistant and in open-circular form (or readily convert to open-circular form). No background signal was detected in *Bgl*II digests obtained from mtDNA-deficient

On the other hand, a higher concentration of H₂O₂ (300 μM) was much less effective at inducing segregation (Figures 1, Cv and D, and Supplemental Figure S2E), presumably due to excess cellular damage. Treatment with 25 or 50 μM H₂O₂ for 30 min did not yield significant changes to m.3243A > G mutant allele content among the measured populations of clones (Figure 1C, ii and iii vs. iv). Therefore only an optimal amount of ROS induced mt-allele segregation toward mutant and wild-type mtDNA homoplasmy during vegetative growth.

Closed circular monomeric mtDNA decreased in H₂O₂-treated MELAS cells

To determine the effects of ROS on mtDNA species, we treated MELAS cells with 100 μM H₂O₂ and performed analysis using one-dimensional gel electrophoresis followed by Southern hybridization. In untreated cells, the closed circular monomer of one genome-unit size is the major species of mtDNA and is converted to a 16.5-kbp linear form upon treatment with *Bam*HI, which has a single cutting site in human mtDNA (Figure 2A). In H₂O₂-treated cells, we observed that closed circular (cc) mtDNA disappeared, and careful examination revealed a faint signal from linear unit-sized mtDNA and other forms in H₂O₂-treated MELAS cells (Figure 2A).

Newly synthesized mtDNA was concatemeric in H₂O₂-treated MELAS cells

Next we sought to elucidate the molecular basis of mt-allelic segregation induced by ROS in human cells. First, we analyzed newly synthesized bromodeoxyuridine (BrdU)-labeled mtDNA by pulsed-field gel-electrophoresis (PFGE), which effectively separates mtDNA molecules from nuclear genomes. We detected BrdU-labeled mtDNA molecules with sizes larger than the unit length from 100 μM H₂O₂-treated MELAS cells but detected only unit-sized mtDNA from untreated cells and no BrdU-signals in ρ⁰ cells (Figure 2B).

To analyze the forms of larger mtDNA, we prepared plugs from cells treated with or without 100 μM H₂O₂ for 30 min followed by various periods of posttreatment cultivation (Supplemental Figure S3). Finally, we subjected the samples to two-dimensional (2D) gel electrophoresis (Figure 3). In untreated cells, primarily open-circular (oc) and cc mtDNA monomers with unit-sized genomes (16.5 kb) were detected as the major mtDNA species (Figure 3i). After treatment with 100 μM H₂O₂ and 1 h of posttreatment cultivation, oc monomers, linear monomers, and fragmented mtDNAs were detectable (Figure 3, ii and iii). After 5 h of posttreatment incubation, fragmented mtDNAs disappeared, oc monomer signals increased, and a faint signal from cc monomers was detected (Figure 3iv). Of note, after 24 h of posttreatment cultivation, linear mtDNA multimers larger than the unit length (>20 kb; concatemers) were detected, and larger amounts of cc monomers were formed (Figure 3v; see also the positions of the size markers in Supplemental Figure S4). Southern blot analysis revealed no remarkable mtDNA signals from ρ⁰ cells, indicating that the signals detected in each panel correspond to mtDNA species (Figure 3vi).

(ρ⁰) cells (lane 4). (B) PFGE profiles of mtDNA. PFGE plugs prepared from MELAS and ρ⁰ cells treated or untreated with H₂O₂, followed by BrdU labeling of mtDNA. Samples were subjected to PFGE along with size and position markers (DNA plugs from *S. cerevisiae*, lambda DNA ladder, 5-kb DNA ladder, supercoiled DNA ladder, and *Bam*HI digest of total DNA from HeLa cells) to indicate the position of unit-sized mtDNA. Whole DNA species (including nuclear species) were visualized by EtBr staining. BrdU-labeled nascent DNA species were detected by immunoblot analysis; larger nascent mtDNA is framed in red.

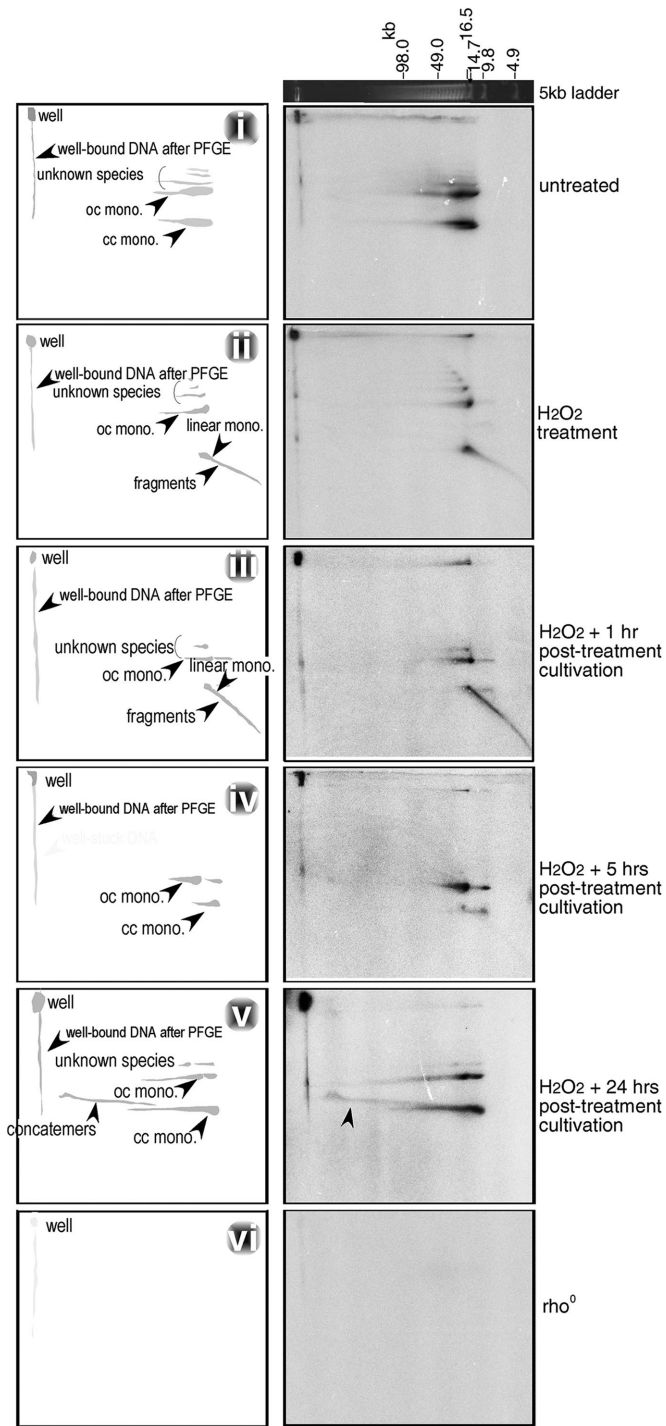


FIGURE 3: Profiles of mtDNA species detected by Southern blot after PFGE-coupled 2D gel electrophoresis. (i–vi) Schematic diagrams indicating mtDNA species corresponding to images on the right showing mtDNA species from MELAS cells treated under the indicated conditions.

These results suggest ROS induced de novo synthesis of multimeric mtDNA species in the treated MELAS cells.

Correlation between concatemer formation and mt-allele segregation

To explore the relationship between concatemer formation and mt-allele segregation from heteroplasmic cells, we designed an assay

system to monitor signal ratios of mtDNA concatemers to nuclear DNA, using PFGE-coupled 2D gel electrophoresis profiles (Figure 4A). Signals from mtDNA and nuclear DNA in cells treated with various concentrations of H₂O₂ followed by 24-h posttreatment incubation were detected by Southern blot analysis using ³²P-labeled DNA fragments from the mtDNA OH region and the nuclear β-actin gene (ACTB), respectively, as probes.

To verify concatemer formation, we excised a piece of agarose gel corresponding to the region predicted to contain linear DNA species with sizes >16.5 kb (Figure 4Aiv, right, red-framed box) after PFGE-coupled 2D gel electrophoresis and isolated the DNA species by digesting the agarose gel with β-agarase I. Large DNA species with branched structures such as the Holliday junction or replication fork-type three-way junctions are unable to enter gels during PFGE and thus should not be included in this linear DNA fraction. The isolated linear DNA was digested with the restriction enzyme *Bam*HI, giving rise to 16.5-kb unit-length fragments (Figure 4B). This result indicates that multimeric mtDNA in H₂O₂-treated MELAS cells are in a head-to-tail configuration and thus are concatemers.

The major mtDNA species in untreated MELAS cells were oc and cc monomers, with nearly undetectable amounts of concatemers, linear monomers, and linear mtDNA fragments <16.5 kbp (Figure 4Ci). Treatment of MELAS cells with 100 μM H₂O₂ followed by 24 h of posttreatment incubation significantly increased concatemer signals (Figure 4Civ) relative to cells treated with lower (75 μM; Figure 4Cii) or higher concentrations of H₂O₂ (150 μM; Figure 4Cv). Concatemer signals were not significant at 50 μM H₂O₂ (Figure 4Cii) and became very faint at >200 μM H₂O₂ (Figure 4C, vi and vii). These results correlate with mt-allele segregation in heteroplasmic cells at the single-cell level (Figure 1C, iv vs. ii, iii, and v). Concatemers are exclusively formed by rolling circle replication or crossing-over-type recombination. Those formed by recombination have discrete lengths (monomers, dimers, trimers, etc.). As shown in Figure 4C, ii–vii, the mtDNA concatemers we detected had continuous lengths and are therefore likely to have been formed by rolling-circle replication.

Detection of rolling-circle replication intermediates from well-bound DNA after PFGE

Concatemers generated by rolling-circle replication are expected to be accompanied by intermediates possessing conjoined circular mtDNA structures at one end. However, some circular structure likely separates from concatemers during experimental processing (Bendich, 1996; Ling and Shibata, 2002, 2004; Ide *et al.*, 2013). In addition, four-way branched structures exist as rolling-circle replication intermediates and may have a role in concatemer-to-monomer resolution (Lewis *et al.*, 2015). DNA species with circular structures, branched DNA with four-way junctions, or replication fork-type three-way junctions (i.e., rolling circle replication intermediates, homologous recombination products, and replication intermediates) are unable to exit PFGE wells but do enter agarose gels during conventional electrophoresis.

We tried to detect rolling-circle replication intermediates (concatemers conjoined with circular mtDNA structures at one end) in samples derived from PFGE wells by two consecutive steps of conventional gel electrophoresis (first through normal agarose and then through low-melting point agarose; schematically illustrated in Figure 5A, i and ii). We isolated DNA species with sizes >16.5 kb from the third electrophoresis round by β-agarase I digestion (Figure 5A, ii, framed in a red box). After *Bam*HI digestion, the isolated DNA yielded a signal corresponding to the unit size (16.5 kb) of mtDNA (Figure 5B), indicating that the mtDNA species that were well bound during PFGE contained concatemers. We also observed that the

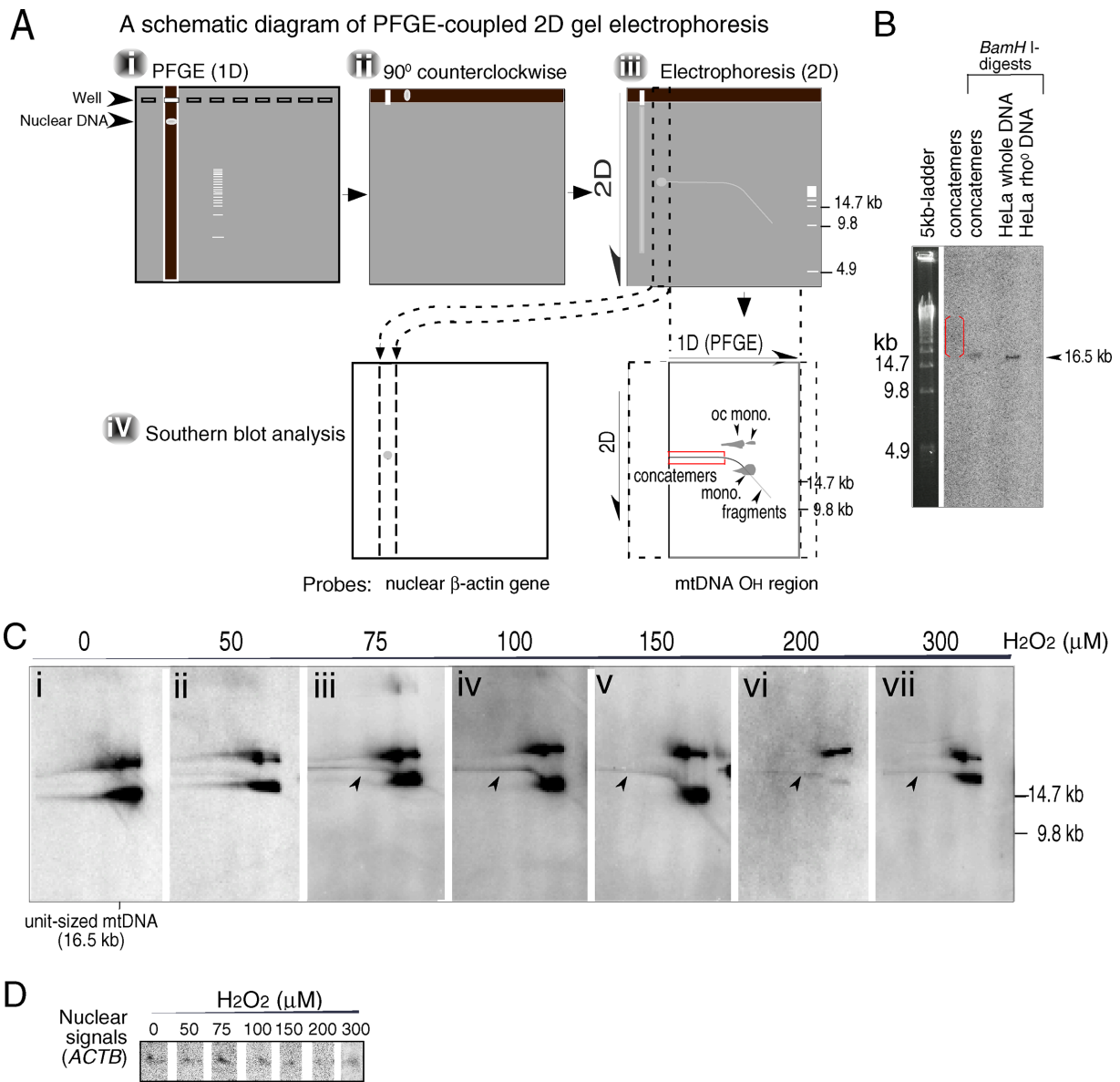


FIGURE 4: Concatemer formation under conditions that induce segregation of the m.3243A > G allele. (A) Schematic diagrams of PFGE-coupled 2D gel electrophoresis of DNA. (i) Plug and marker run in the first dimension. (ii) Excised lane of total cellular DNA, rotated 90° counterclockwise and embedded in a newly poured gel for 2D electrophoresis. (iii) DNA species after EtBr staining. (iv) Left and right, nuclear DNA after 2D electrophoresis and mtDNA species separated from the nuclear chromosomes and well-bound DNAs after undergoing PFGE, respectively. Signals from mtDNA and nuclear DNA were detected by Southern hybridization. Arrowheads indicate the positions of each mtDNA species (bottom right). (B) Identification of head-to-tail concatemers. Gel containing the concatemers (framed in a red box; see Aiv) was excised. Purified DNA was divided into two equal parts for the undigested control and *Bam*HI-digested samples. Arrowhead indicates the position of unit-sized mtDNA. (C, D) Signals from mtDNA (C) and nuclear DNA (D) from cells treated with the indicated concentration of H₂O₂.

*Bgl*II-digested sample contained well-bound DNA species, using conventional gel electrophoresis (Figure 5B), which had previously been excised from a low-melting point agarose gel after PFGE-coupled 2D electrophoresis, leading us to infer that the large isolated mtDNA species contain impurities from the gel and thus tend to form aggregates spontaneously during DNA handling. On the other hand, because exonuclease III (ExoIII) digests double-stranded DNA in the 3' to 5' direction starting from the 3'-OH end, we predicted that ExoIII treatment would allow for migration of species with attached linear DNA. Digestion of well-bound DNA obtained after the first PFGE run with ExoIII (Kusano *et al.*, 1989) generated

signals from circular monomers, which were able to enter the gel during the second PFGE run (Figure 5, C and D). These results indicate that circular structures with attached linear DNAs were among the well-bound DNA species.

Induced endogenous ROS generation promoted mt-allele segregation

Next we set out to examine whether inducing endogenous ROS production can also lead to mt-allele segregation. MtDNA polymerase γ (POLG) is essential for replication and repair of mtDNA. Inhibition of POLG by ethidium bromide (EtBr) treatment depletes mtDNA

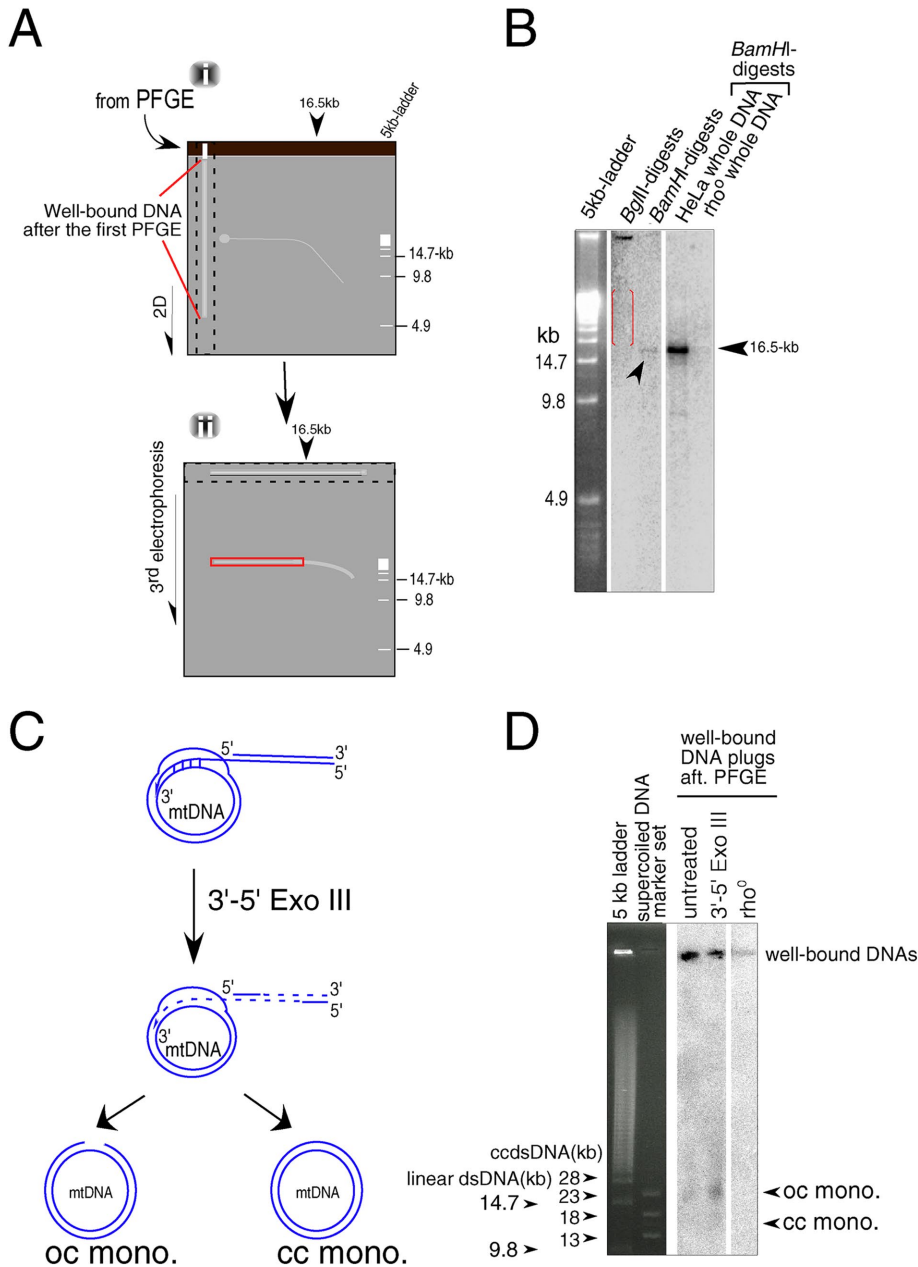


FIGURE 5: Detection of rolling-circle replication intermediates from well-bound DNA after PFGE. (A) Procedure for identifying species of mtDNA after PFGE-coupled 2D electrophoresis. We ran PFGE using plugs prepared from MELAS cells treated with 100 μM H_2O_2 for 0.5 h and then cultured for 24 h. The 2D gel electrophoresis runs were performed to allow well-bound DNA to enter the gel (top). Gel containing the well-bound DNAs after PFGE (framed with black dashed lines) was excised, rotated 90° counterclockwise, embedded in a newly poured 1% low-melting point agarose gel, and subjected to a second round of electrophoresis (bottom). DNA species with sizes >16.5 kb (framed with a red box) were cut out and purified after the gel was digested with β -agarase. (B) Restriction enzyme digestion of the predicted concatemeric mtDNAs. Purified DNA molecules were separated into two parts: the first aliquot was digested with *Bgl*II to reduce the possible effects of contaminating nonspecific nuclear DNA signals to a minimum. The second aliquot was digested with *Bam*HI. Positions of unit-sized mtDNA are indicated by arrowheads. (C) Schematic diagram of 3'-5' digestion of rolling-circle intermediates by ExoIII to generate open (oc mono.) and closed-circular (cc mono.) monomers. Broken lines indicate the digested DNA strands. (D) After undergoing the first PFGE run, the DNA plugs containing well-bound DNAs were divided into two smaller plugs of nearly identical dimensions. ExoIII-treated and untreated plugs were subjected to a second PFGE run. MtDNA signals were detected by Southern blot analysis.

(Okamaoto *et al.*, 2003) and induces endogenous ROS production (Palmeira *et al.*, 2007; Sasaki *et al.*, 2008). We hypothesized that ROS contribute to mt-allele segregation from heteroplasmy toward homoplasmy upon copy number reduction in heteroplasmic MELAS cell cultures. To test this possibility, we treated MELAS cells with EtBr for 6 d, thereby decreasing mtDNA copy number to <10% of control levels (Figure 6A). Using a flow cytometer and the fluorogenic dye MitoSOX red, an indicator for mitochondrial superoxide in live cells (Robinson *et al.*, 2006), we detected increased ROS levels at 3 and 6 d after EtBr treatment (Figure 6, A and B). Subsequent washing and incubation for 6 d allowed for recovery of mtDNA copy number to a mean value of 79.7% of control levels (Figure 6A) and a decrease in ROS levels to those of untreated MELAS cells at 3 and 6 d after washing out EtBr (Figure 6B). After the recovery process, the m.3243A > G mutant fraction exhibited a much wider distribution (Figure 6Cii and Supplemental Figure S5B), indicating mt-allele segregation.

To further examine the role of ROS in EtBr induced mt-allele segregation, we also treated MELAS cells with EtBr in the presence of ROS scavenger vitamin C or N-acetylcysteine (NAC), respectively. Vitamin C partially but significantly inhibited mt-allele segregation toward lower mutant-allele frequency in EtBr-treated MELAS cells (Figure 6, C, ii vs. iv, and D, and Supplemental Figure S5, B vs. C). In the presence of NAC, we also observed broadening of the distribution of the m.3243A > G mutant fraction (Figure 6, C, ii vs. iii, and D, and Supplemental Figure S5, B vs. C). NAC treatment increases the intracellular level of glutathione, an antioxidant and substrate of glutathione peroxidase. Because EtBr inhibits glutathione peroxidase activity in EtBr-treated rat brains (Abdel-Salam *et al.*, 2012), we suspected that the poor efficacy of NAC was due to inhibition of glutathione peroxidase activity by EtBr. No broadening in the distribution of the m.3243A > G mutant fraction occurred in clones treated with either NAC or vitamin C alone (Figure 6, C, i vs. v and i vs. vi, and Supplemental Figure S5, A vs. E or F). It is very likely that a decrease in mtDNA-encoded electron transport chain (ETC) subunits affected the balance in the relative abundance between the nuclear- and mitochondrial-encoded subunits, thereby disrupting formation of ETC complexes and causing endogenous ROS production.

On the basis of the foregoing observations, we propose a model in which ROS

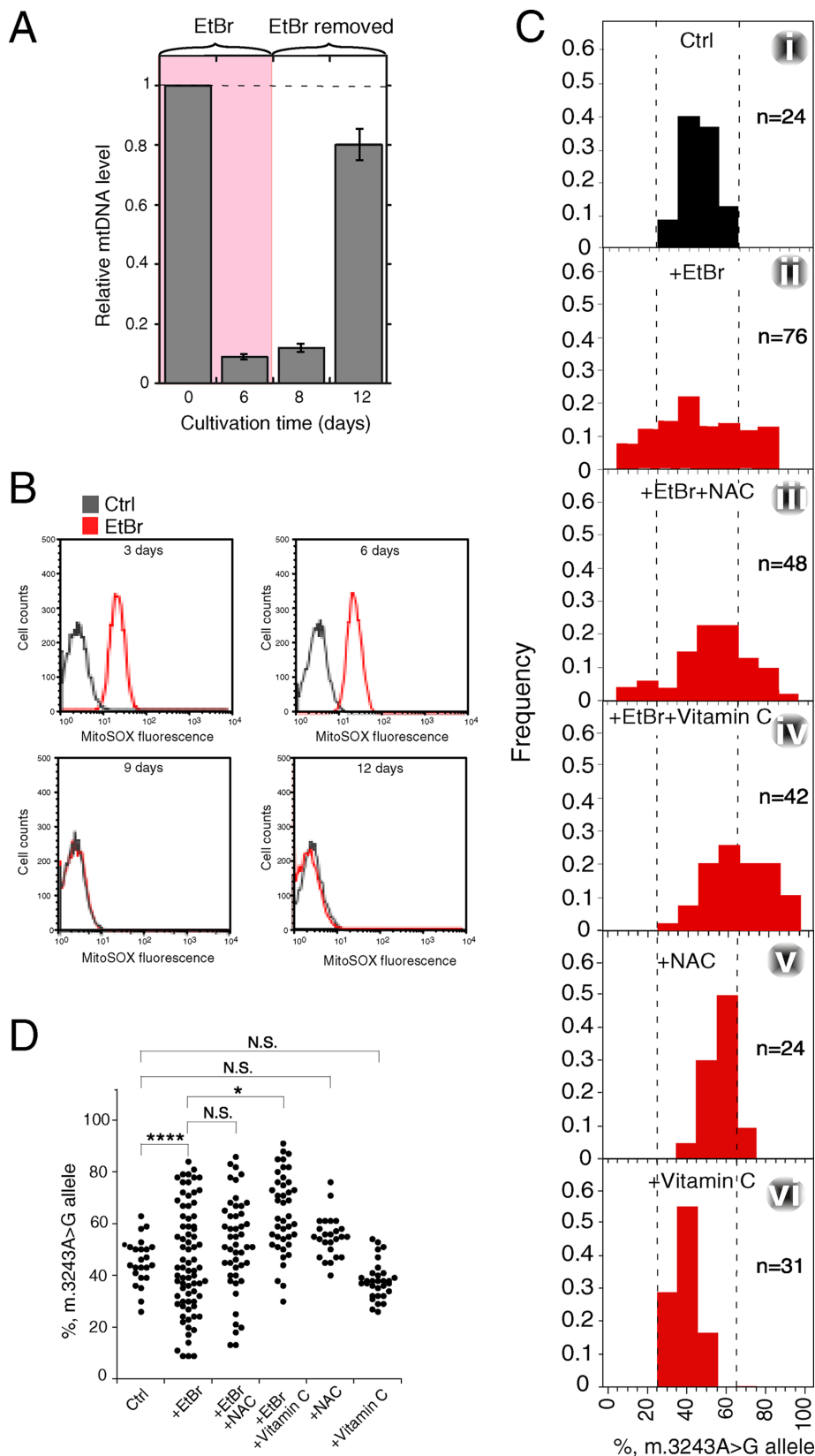


FIGURE 6: Segregation of mt-alleles in heteroplasmic MELAS cells upon endogenous ROS induction. The experimental procedure is shown in Supplemental Figure S1B. (A) Changes in mtDNA copy number upon EtBr treatment. MELAS cells were treated with 50 ng/ml EtBr for 6 d and then allowed to recover for 6 d. Total DNA was extracted, and relative mtDNA copy number was determined by real-time PCR analysis in triplicate at the indicated time points. (B) Increases in ROS level upon EtBr treatment. MELAS cells were treated with 50 ng/ml EtBr for

production decreases the amount of intact closed-circular mtDNA monomers (potential replication templates) while triggering rolling circle replication on a few residual templates to generate head-to-tail multimers (concatemers) with the same sequence as the template circular DNA. The resulting concatemer formation allows for inheritance of a number of mtDNA genome units into sister cells as a single segregation unit and thus stimulates mtDNA-allele segregation toward wild-type and mutant mtDNA homoplasmy through clonal expansion (Figure 7).

DISCUSSION

In this study, we presented evidence that an optimal level of ROS promoted segregation of heteroplasmic alleles of mtDNA in human cells, and this segregation correlated with the ROS-promoted synthesis of linear tandem multimers (concatemers), which were products of rolling-circle replication. Thus the mechanism for homoplasmy restoration is likely evolutionarily conserved in human mitochondria.

Treatment of human cells with H_2O_2 causes oxidative damage to DNA bases and mainly results in single-stranded (ss) breaks (Rueff *et al.*, 1993; Villani *et al.*, 2010). Of note, we observed the disappearance of cc mtDNA (Figure 2A) and fragmentation (Figure 3, ii and iii) in H_2O_2 -treated MELAS cells, which contributes to the generation of double-strand breaks (DSBs) in mtDNA molecules. Subsequent processing of newly formed DSBs by a 5'-3' exonuclease would generate 3'-ssDNA tails, which are known substrates for heteroduplex joint formation directed by a homologous DNA pairing protein. These 3' ssDNA tails of mtDNA fragments would then be used to initiate rolling-circle replication as in budding yeast (for reviews, see Solieri, 2010; Chen, 2013).

6 d. After EtBr removal, cells were then allowed to recover for 6 d. Relative ROS levels at the indicated time points were analyzed by MitoSOX labeling. (C) Segregation of mtDNA alleles by EtBr treatment. Distribution of the m.3243A > G mutant fraction in clones derived from (i) untreated (Ctrl) cells, (ii) EtBr-treated cells, (iii) EtBr-treated cells cultivated in the presence of NAC or (iv) vitamin C, and (v, vi) Ctrl cells cultivated in the presence of (v) NAC or (vi) vitamin C alone. (D) Statistical analysis for distribution of the m.3243A > G mutant fraction in clones derived from cells under the conditions described in C. *, $p < 0.05$; ****, $p < 0.0001$; N.S., not significant.

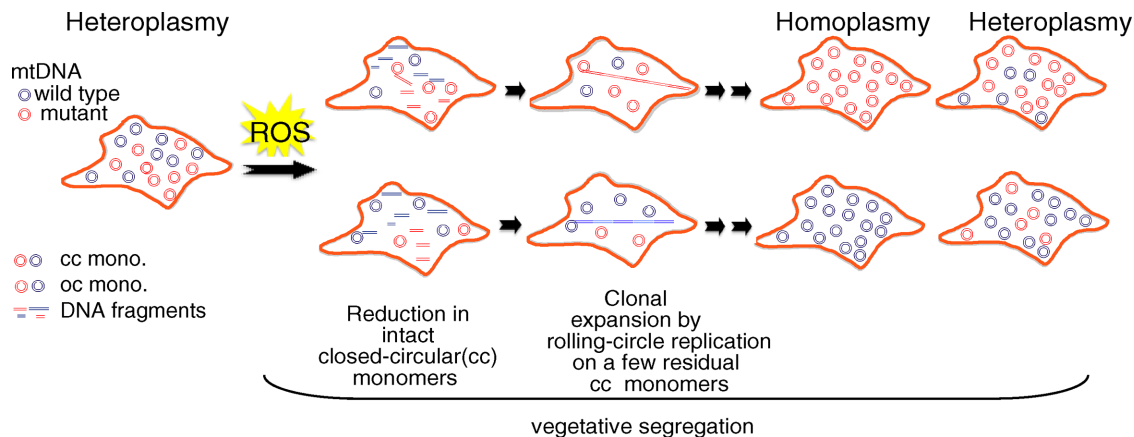


FIGURE 7: Model for ROS-induced segregation of mtDNA alleles. ROS cause a decrease in amounts of intact closed-circular mtDNA monomers, which serve as templates for rolling-circle replication. Rolling-circle replication is initiated by an invading 3'-single-stranded terminus derived from a fragmented mtDNA, as in the case of yeast mitochondria (Ling and Shibata, 2004; Ling et al., 2007, 2011), and generates concatemers consisting of a number of identical sequences. The resulting concatemers allow for inheritance of a number of mtDNA genome units into sister cells as a single segregation unit and thus stimulate mt-allele segregation toward wild-type or mutant mtDNA homoplasmity.

On the other hand, H_2O_2 treatment causes mtDNA damage, which results in a greatly reduced number of cc monomeric mtDNAs remaining intact (Figures 2A and Figure 3ii). These results suggest that the reduced mtDNA copy number is responsible, at least in part, for inducing mt-allele segregation. Of importance, mathematical modeling predicted that decreasing the number of mtDNA-segregating units to a few copies would promote the segregation of mt-alleles (Birky, 1978a,b). However, human fibroblast cells each contain ≥ 1000 copies of mtDNA (Lehtinen et al., 2000). Although EtBr treatment reduces mtDNA copy number to 1/10 of the initial level (Figure 6A), ≥ 100 copies of mtDNA would still remain.

Indeed, we found that treatment with EtBr induced ROS production and promoted mt-allele segregation (Figure 6, A and C). In addition, ROS scavengers such as vitamin C partially but significantly impaired mt-allele segregation in EtBr-treated MELAS cells (Figure 6, Civ and D, and Supplemental Figure S5D). These results suggest that ROS play a role in the observed mt-allele segregation. The results taken together indicate that decreasing copy number alone is not sufficient to explain the observed segregation; in other words, reduction in mtDNA replication templates coupled with concatemer formation contributes to mt-allele segregation.

Rapid segregation of heteroplasmic mtDNA occurs at the genetic bottleneck, which is accompanied by remarkable decreases in mtDNA level during oogenesis and increases in mtDNA level during folliculogenesis (Cree et al., 2008; Khrapko, 2008; Wai et al., 2008). Folliculogenesis is regulated by various hormones, including estrogens such as estradiol (Roche, 1996), which induces ROS production at a high level (Okoh et al., 2011). We infer that ROS-mediated concatemer formation might contribute to increases in mtDNA content during folliculogenesis.

In summary, this study, in conjunction with our previous studies in budding yeast (for reviews, see Solieri, 2010; Ling et al., 2011; Chen, 2013), provides new insights into the mechanism underpinning homoplasmity restoration in mammalian cells.

MATERIALS AND METHODS

Cells, cell culture, and reagents

Primary heteroplasmic fibroblast cell lines containing m.3243A > G mutant mtDNA derived from different MELAS patients were

obtained from the fibroblast repository at the National Center of Neurology and Psychiatry (NCNP; Tokyo, Japan) under written informed consent and with the approval of the NCNP Institutional Review Board.

Cells were maintained in DMEM (Wako Pure Chemical Industry, Osaka, Japan) supplemented with 10% fetal bovine serum and penicillin/streptomycin (100 U/ml and 100 mg/ml, respectively) at 37°C in a humidified incubator in an atmosphere containing 5% CO_2 . Pyruvate (100 μ g/ml) and uridine (50 μ g/ml) were added to the culture medium to allow growth of rho⁻ or rho⁰ cells generated after chemical treatment.

DNA plugs from *S. cerevisiae*, lambda ladder, and 5-kb DNA ladder were purchased from Bio-Rad Laboratories (Tokyo, Japan). Supercoiled DNA ladder and supercoiled DNA marker sets were purchased from Invitrogen and Epicentre, respectively. These DNA size markers were used as references for the sizes and positions of DNA species.

Southern blot analysis for detection of nuclear DNA and mtDNA molecules

Total cellular DNA (~15 μ g) was separated by electrophoresis on a 0.5% agarose gel, run at 4°C for 30 h at 1 V/cm, and transferred to a nylon membrane (Amersham Hybond N Plus; GE Healthcare). Signals for mtDNA were detected using the ³²P-labeled mtDNA OH region as a probe, as described (Anderson et al., 1981; Lehtinen et al., 2000). Signals for nuclear DNA were detected using a ³²P-labeled DNA fragment of the β -actin gene, *ACTB* (for nuclear DNA), as a probe. Primers designed for the mtDNA OH region were forward, 5'-TAACCACTCACGGGAGCTCT-3', and reverse, 5'-AAGGC-TAGGACCAAACCTAT-3'. Primers designed for *ACTB* were forward, 5'-TGCGTGACATTAAGGAGAAGCTGTGC-3', and reverse, 5'-CTC-GTCATACTCCTGCTTGCTGATCC-3'. Signals corresponding to mtDNA and nuclear DNA fragments were quantitated using a Fujifilm BAS-2500 image analyzer (Fujifilm, Tokyo, Japan).

Treatment with chemical compounds and single-cell cloning

Cells were plated at 30–50% confluence 1 d before treatment with chemical compounds. After treatment, cells were allowed to recover in fresh medium for 6 d and then plated at high dilution to create

isolated colonies. Colonies derived from single cells were then collected using cloning rings.

Measurement of intracellular ROS

The intracellular ROS level after H₂O₂ treatment was measured by use of 5-(and-6)-chloromethyl-2,7-dichlorodihydrofluorescein diacetate acetyl ester (CM-H2DCFDA; Molecular Probes, Nacalai Tesque, Kyoto, Japan). Cells (1×10⁵/ml) were first incubated with 10 μM CM-H2DCFDA for 15 min at 37°C and then treated with H₂O₂ and analyzed kinetically in a SpectraMax microplate reader (Molecular Devices, Sunnyvale, CA).

Measurement of ROS after EtBr treatment was performed by flow cytometer. After EtBr treatment, ~1 × 10⁶ cells were trypsinized and each cell pellet was resuspended in 1× phosphate-buffered saline (PBS) containing 5 μM MitoSOX (Molecular Probes, M36008). ROS levels were then analyzed by flow cytometry at the Research Resources Center, RIKEN Brain Science Institute (Wako, Japan).

DNA preparation and a PCR-RFLP assay for m.3243A > G-heteroplasmy

The heteroplasmy level was estimated by the m.3243A > G mutant fraction, measured using the PCR-RFLP assay described by Goto *et al.* (1990). Briefly, a 294–base pair mtDNA region containing np 3243 was amplified by PCR using a forward primer (5′-AG-GACAAGAGAAATAAGGCC; nps 3130–3149), a reverse primer (5′-ACGTTGGGGCCTTTGCGTAG; nps 3423–3404), and whole cellular DNA as a template. The *Apal* digests (182– and 112–base pair mtDNA fragments) of the purified PCR products were separated on a 2% agarose gel by electrophoresis and detected by Southern hybridization using an [α-³²P]dCTP-labeled 294–base pair DNA fragment as a probe. Signals were quantitatively analyzed using a FujiFilm BAS-2500 image analyzer. The m.3243A > G mutant fraction was calculated as the proportion of the signals from the 182– and 112–base pair mtDNA fragments to the total signals from the uncut 294–, 182–, and 112–base pair mtDNA fragments.

Statistical analysis

The *F* test was used to determine the statistical significance of differences in the distributions of m.3243A > G allele frequency between two independent groups.

DNA extraction and real-time PCR for mtDNA copy-number analysis

Total cellular DNA was extracted using the DNAzol Reagent (Invitrogen). Relative mtDNA copy number was defined as the ratio of mtDNA (represented by the ND1 gene) to nuclear DNA (represented by the β-actin gene). Primers for the ND1 gene were forward, 5′-CCCTAAAACCCGCGCACATCT-3′, and reverse, 5′-GAGC-GATGGTGAGAGCTAAGGT-3′. Primers for the ACTB gene were as in the Southern blot analysis. Mitochondrial and nuclear primer sets were run for each sample in triplicate. Various dilutions of the template DNA were used in the PCR reaction to ensure that measurements were within the linear range of the assay.

Analyses of mtDNA by PFGE

For preparation of plugs for PFGE, cells were suspended in 100 μl of Tris-EDTA buffer (0.5 M EDTA, 10 mM Tris, pH 7.5) and mixed well by pipetting with 250 μl of 1.6% low-melting point agarose (made in an EDTA/Tris solution containing 50 mM EDTA, 10 mM Tris, pH 7.5). The suspension was added to a DR11 sample mold

(170-3622; Bio-Rad, Hercules, CA) to form plugs on ice for 10–20 min. Each plug was transferred to a 15 ml of Corning centrifuge tube containing 2 ml of lysis buffer (0.5 M EDTA, 10 mM Tris, 1% N-lauroylsarcosine, pH 9.5) suspended with 2 μg/ml proteinase K (Merck) and incubated at 50°C overnight. Before PFGE, the plugs were washed with EDTA/Tris solution. PFGE was performed with a contour-clamped homogeneous electric field instrument (Bio-Rad CHEF DR11). The running conditions were 6 V/cm at 14°C for 11 h, initial and final intervals 2 and 12 s, respectively, in 0.5× TBE buffer (1× TBE is 0.089 M Tris, 0.089 M boric acid, 0.002 M EDTA).

Labeling of nascent mtDNA

MELAS and p⁰ cells were untreated or treated with 100 μM H₂O₂ for 0.5 h after incubation with BrdU for 30 min. After washing, the nascent mtDNA was labeled by growing cells for 24 h in fresh medium containing 10 μM BrdU (Sigma-Aldrich). For preparation of each PFGE plug, cells were washed with PBS buffer to remove BrdU, resuspended in 50 μl Tris-EDTA buffer (0.5 M EDTA, 10 mM Tris, pH 7.5), and then mixed well by pipetting with 150 μl of 1.6% low-melting point agarose at 50°C. PFGE plugs were formed by adding the suspension to a Bio-Rad DR11 sample mold.

PFGE-coupled 2D gel electrophoretic analyses

After PFGE, the desired DNA-containing gel segment was excised, rotated 90° counterclockwise, and embedded in a newly poured 1% agarose gel. The DNA was then subjected to 2D gel electrophoretic analyses as previously described (Brewer and Fangman, 1987; Ling and Shibata, 2004; Ling *et al.*, 2007). A 5-kbp DNA ladder (Bio-Rad) was used as a size marker. The 2D run was performed at 5 V/cm on a 1% agarose gel or 1% low-melting point gel (for purifying the DNA species) in TBE buffer with 0.3 μg/ml EtBr at 4°C. Signals for mtDNA and nuclear DNA were detected by Southern hybridization using the ³²P-labeled mtDNA OH region or the ³²P-labeled DNA fragment of the β-actin gene as a probe.

Exonuclease digestion

DNA plugs with dimensions of 1 × 2 × 0.15 cm were prepared from 1 × 10⁷ MELAS cells treated with 100 μM H₂O₂ for 0.5 h, cultured for 24 h, and then subjected to PFGE. Plugs containing well-bound DNAs were taken from PFGE wells and divided into two smaller plugs (with dimensions of 1 × 0.5 × 0.15 cm). One plug was soaked in 1× ExoIII buffer without addition of the corresponding exonuclease as a control. The remaining plug was soaked in 1× ExoIII buffer. Exonuclease digestion of each smaller plug was performed at 37°C for 15 h (Kusano *et al.*, 1989). ExoIII with attached buffer was purchased from NEB.

ACKNOWLEDGMENTS

We deeply appreciate Elliot Bradshaw, Chemical Genetics Laboratory, RIKEN, for proofreading the manuscript. This work was supported in part by a Grant-in-Aid for Scientific Research (C) (26440013) from the Ministry of Education, Culture, Sports, Science and Technology of Japan to F.L., an Incentive Research Grant from RIKEN to F.L., a grant from the RIKEN Strategic Research Program, and a grant from the Japan Agency for Medical Research and Development–Core Research for Evolutional Science and Technology to F.L.

REFERENCES

Abdel-Salam OM, Khadrawy YA, Mohammed NA, Youness ER (2012). The effect of gabapentin on oxidative stress in a model of toxic demyelination in rat brain. *J Basic Clin Physiol Pharmacol* 23, 61–68.

- Anderson S, Bankier AT, Barrell BG, de Bruijn MH, Coulson AR, Drouin J, Eperon IC, Nierlich DP, Roe BA, Sanger F, *et al.* (1981). Sequence and organization of the human mitochondrial genome. *Nature* 290, 457–465.
- Ashley MV, Laipis PJ, Hauswirth WW (1989). Rapid segregation of heteroplasmic bovine mitochondria. *Nucleic Acids Res* 17, 7325–7331.
- Bendich AJ (1996). Structural analysis of mitochondrial DNA molecules from fungi and plants using moving pictures and pulsed-field gel electrophoresis. *J Mol Biol* 255, 564–588.
- Bienert GP, Schjoerring JK, Jahn TP (2006). Membrane transport of hydrogen peroxide. *Biochim Biophys Acta* 1758, 994–1003.
- Birky CW Jr (1978a). Transmission genetics of mitochondria and chloroplasts. *Annu Rev Genet* 12, 471–512.
- Birky CW Jr, Strausberg RL, Forster JL, Perlman PS (1978b). Vegetative segregation of mitochondria in yeast: estimating parameters using a random model. *Mol Gen Genet* 158, 251–261.
- Brewer BJ, Fangman WL (1987). The localization of replication origins on ARS plasmids in *S. cerevisiae*. *Cell* 51, 463–471.
- Cao L, Shitara H, Horii T, Nagao Y, Imai H, Abe K, Hara T, Hayashi J, Yonekawa H (2007). The mitochondrial bottleneck occurs without reduction of mtDNA content in female mouse germ cells. *Nat Genet* 39, 386–390.
- Chen XJ (2013). Mechanism of homologous recombination and implications for aging-related deletions in mitochondrial DNA. *Microbiol Mol Biol Rev* 77, 476–496.
- Cree LM, Samuels DC, de Sousa Lopes SC, Rajasimha HK, Wonnapijit P, Mann JR, Dahl HH, Chinnery PF (2008). A reduction of mitochondrial DNA molecules during embryogenesis explains the rapid segregation of genotypes. *Nat Genet* 40, 249–254.
- Fujikura J, Nakao K, Sone M, Noguchi M, Mori E, Naito M, Taura D, Harada-Shiba M, Kishimoto I, Watanabe A, *et al.* (2012). Induced pluripotent stem cells generated from diabetic patients with mitochondrial DNA A3243G mutation. *Diabetologia* 55, 1689–1698.
- Goto Y, Nonaka I, Horai S (1990). A mutation in the tRNA(Leu)(UUR) gene associated with the MELAS subgroup of mitochondrial encephalomyopathies. *Nature* 348, 651–653.
- Hauswirth WW, Laipis PJ (1982). Mitochondrial DNA polymorphism in a maternal lineage of Holstein cows. *Proc Natl Acad Sci USA* 79, 4686–4690.
- Holt IJ, Harding AE, Morgan-Hughes JA (1988). Deletions of muscle mitochondrial DNA in patients with mitochondrial myopathies. *Nature* 331, 717–719.
- Ide S, Saka K, Kobayashi T (2013). Rtt109 prevents hyper-amplification of ribosomal RNA genes through histone modification in budding yeast. *PLoS Genet* 9, e1003410.
- Kadowaki T, Kadowaki H, Mori Y, Tobe K, Sakuta R, Suzuki Y, Tanabe Y, Sakura H, Awata T, Goto Y, *et al.* (1994). A subtype of diabetes mellitus associated with a mutation of mitochondrial DNA. *N Engl J Med* 330, 962–968.
- Kamata H, Hirata H (1999). Redox regulation of cellular signalling. *Cell Signal* 11, 1–14.
- Khrapko K (2008). Two ways to make an mtDNA bottleneck. *Nat Genet* 40, 134–135.
- Koehler CM, Lindberg GL, Brown DR, Beitz DC, Freeman AE, Mayfield JE, Myers AM (1991). Replacement of bovine mitochondrial DNA by a sequence variant within one generation. *Genetics* 129, 247–255.
- Kusano K, Nakayama K, Nakayama H (1989). Plasmid-mediated lethality and plasmid multimer formation in an *Escherichia coli* recBC sbcBC mutant. Involvement of RecF recombination pathway genes. *J Mol Biol* 209, 623–634.
- Lehtinen SK, Hance N, El Meziane A, Juhola MK, Juhola KM, Karhu R, Spelbrink JN, Holt IJ, Jacobs HT (2000). Genotypic stability, segregation and selection in heteroplasmic human cell lines containing np 3243 mutant mtDNA. *Genetics* 154, 363–380.
- Lewis SC, Joers P, Willcox S, Griffith JD, Jacobs HT, Hyman BC (2015). A rolling circle replication mechanism produces multimeric lariats of mitochondrial DNA in *Caenorhabditis elegans*. *PLoS Genet* 11, e1004985.
- Ling F, Hori A, Shibata T (2007). DNA recombination-initiation plays a role in the extremely biased inheritance of yeast [rho-] mitochondrial DNA that contains the replication origin ori5. *Mol Cell Biol* 27, 1133–1145.
- Ling F, Mikawa T, Shibata T (2011). Enlightenment of yeast mitochondrial homoplasmy: diversified roles of gene conversion. *Genes (Basel)* 2, 169–190.
- Ling F, Shibata T (2002). Recombination-dependent mtDNA partitioning: in vivo role of Mhr1p to promote pairing of homologous DNA. *EMBO J* 21, 4730–4740.
- Ling F, Shibata T (2004). Mhr1p-dependent concatemeric mitochondrial DNA formation for generating yeast mitochondrial homoplasmic cells. *Mol Biol Cell* 15, 310–322.
- Linnane AW, Marzuki S, Ozawa T, Tanaka M (1989). Mitochondrial DNA mutations as an important contributor to ageing and degenerative diseases. *Lancet* 333, 642–645.
- Neill S, Desikan R, Hancock J (2002). Hydrogen peroxide signalling. *Curr Opin Plant Biol* 5, 388–395.
- Okamoto M, Ohsato T, Nakada K, Isoe K, Spelbrink JN, Hayashi J, Hamasaki N, Kang D (2003). Ditercalinium chloride, a pro-anticancer drug, intimately associates with mammalian mitochondrial DNA and inhibits its replication. *Curr Genet* 43, 364–370.
- Okoh V, Deoraj A, Roy D (2011). Estrogen-induced reactive oxygen species-mediated signalings contribute to breast cancer. *Biochim Biophys Acta* 1815, 115–133.
- Ozawa T (1997). Genetic and functional changes in mitochondria associated with aging. *Physiol Rev* 77, 425–464.
- Palmeira CM, Rolo AP, Berthiaume J, Bjork JA, Wallace KB (2007). Hyperglycemia decreases mitochondrial function: the regulatory role of mitochondrial biogenesis. *Toxicol Appl Pharmacol* 225, 214–220.
- Raap AK, Jahangir Tafrechi RS, van de Rijke FM, Pyle A, Wahlby C, Szuhai K, Ravelli RB, de Coo RF, Rajasimha HK, Nilsson M, *et al.* (2012). Non-random mtDNA segregation patterns indicate a metastable heteroplasmic segregation unit in m.3243A>G hybrid cells. *PLoS One* 7, e52080.
- Reardon W, Ross RJ, Sweeney MG, Luxon LM, Pembrey ME, Harding AE, Trembath RC (1992). Diabetes mellitus associated with a pathogenic point mutation in mitochondrial DNA. *Lancet* 340, 1376–1379.
- Robinson KM, Janes MS, Pehar M, Monette JS, Ross MF, Hagen TM, Murphy MP, Beckman JS (2006). Selective fluorescent imaging of superoxide in vivo using ethidium-based probes. *Proc Natl Acad Sci USA* 103, 15038–15043.
- Roche JF (1996). Control and regulation of folliculogenesis—a symposium in perspective. *Rev Reprod* 1, 19–27.
- Rueff J, Bras A, Cristovao L, Mexia J, Sa da Costa M, Pires V (1993). DNA strand breaks and chromosomal aberrations induced by H₂O₂ and ⁶⁰Co gamma-radiation. *Mutat Res* 289, 197–204.
- Sasaki R, Suzuki Y, Yonezawa Y, Ota Y, Okamoto Y, Demizu Y, Huang P, Yoshida H, Sugimura K, Mizushima Y (2008). DNA polymerase gamma inhibition by vitamin K3 induces mitochondria-mediated cytotoxicity in human cancer cells. *Cancer Sci* 99, 1040–1048.
- Smeitink JA, Zeviani M, Turnbull DM, Jacobs HT (2006). Mitochondrial medicine: a metabolic perspective on the pathology of oxidative phosphorylation disorders. *Cell Metab* 3, 9–13.
- Solieri L (2010). Mitochondrial inheritance in budding yeasts: towards an integrated understanding. *Trends Microbiol* 18, 521–530.
- Villani P, Eleuteri P, Grollino MG, Rescia M, Altavista P, Spano M, Pacchierotti F, Cordelli E (2010). Sperm DNA fragmentation induced by DNase I and hydrogen peroxide: an in vitro comparative study among different mammalian species. *Reproduction* 140, 445–452.
- Wai T, Teoli D, Shoubridge EA (2008). The mitochondrial DNA genetic bottleneck results from replication of a subpopulation of genomes. *Nat Genet* 40, 1484–1488.
- Wallace DC (1994). Mitochondrial DNA sequence variation in human evolution and disease. *Proc Natl Acad Sci USA* 91, 8739–8746.